Mon. Not. R. Astron. Soc. **000**, 1–**??** (2013) Printed 8 December 2015 (MN LATEX style file v2.2)

The Epoch of Reionization in the $R_h = ct$ Universe

Fulvio Melia[1⋆] and Marco Fatuzzo[2†]

[1]*Department of Physics, The Applied Math Program, and Department of Astronomy, The University of Arizona, AZ 85721, USA*

[2]*Physics Department, Xaiver University, Cincinnati, OH 45207*

ABSTRACT

The measured properties of the epoch of reionization (EoR) show that reionization probably began around $z \sim 12 - 15$ and ended by $z = 6$. In addition, a careful analysis of the fluctuations in the cosmic microwave background indicate a scattering optical depth $\tau \sim 0.066 \pm 0.012$ through the EoR. In the context of ΛCDM, galaxies at intermediate redshifts and dwarf galaxies at higher redshifts now appear to be the principal sources of UV ionizing radiation, but only for an inferred (ionizing) escape fraction $f_{ion} \sim 0.2$, which is in tension with other observations that suggest a value as small as ~ 0.05. In this paper, we examine how reionization might have progressed in the alternative Friedmann-Robertson Walker cosmology known as the $R_{\rm h} = ct$ Universe, and determine the value of f_{ion} required with this different rate of expansion. We find that $R_{\rm h} = ct$ accounts quite well for the currently known properties of the EoR, as long as its fractional baryon density falls within the reasonable range $0.026 \lesssim \Omega_b \lesssim 0.037$. This model can also fit the EoR data with $f_{ion} \sim 0.05$, but only if the Lyman continuum photon production is highly efficient and $\Omega_b \sim 0.037$. These results are still preliminary, however, given their reliance on a particular form of the star-formation rate density, which is still uncertain at very high redshifts. It will also be helpful to reconsider the EoR in $R_{\rm h} = ct$ when complete structure formation models become available.

Key words: cosmological parameters, cosmology: observations, cosmology: theory, early universe, galaxies: general, quasars: general

⋆ John Woodruff Simpson Fellow. E-mail: fmelia@email.arizona.edu
† E-mail: fatuzzo@xavier.edu

1 INTRODUCTION

In the standard model of cosmology, the Universe entered the so-called "dark ages" soon after recombination, at cosmic time $t \sim 380,000$ years, initiating a period that ended only when stars and galaxies began forming some 400 Myr later (Barkana & Loeb 2001; Bromm & Larson 2004). It is thought that during the ensuing ~ 500 Myrs, Lyman continuum radiation from early galaxies and emerging active galactic nuclei (AGNs) reionized the expanding gas, producing a fully ionized intergalactic medium (IGM) by redshift $z \sim 6$. This termination point is well established observationally, e.g., through the Gunn-Peterson absorption measured in high-redshift quasars, whose spectra reveal that hydrogen was highly ionized by $t \sim 1$ Gyr (e.g., Songaila 2004; Fan et al. 2006). And while the precise time (or redshift) at which the Epoch of Reionization (EoR) began is not as well established, indications from, e.g., the cosmic microwave background (CMB) polarization data, are that it probably began no later than $z \sim 10-15$ (Jarosik et al. 2011; Hinshaw et al. 2013).

But though it is generally understood that the IGM was ionized by the integrated UV field from AGNs and star-forming galaxies (Miralda-Escude & Ostriker 1990; Haardt & Madau 1996), the relative contributions from them, or even which dominated the UV emission first or last, are issues that have not yet been fully resolved. Recent work constraining HI reionization by high-redshift AGNs, based on observed limits to the unresolved X-ray background (Haardt & Salvaterra 2015), suggests that to avoid over-producing the X-ray signal measured at $z = 0$, such quasars could not have been responsible for more than $\sim 13\%$ of the HII filling factor by $z \sim 6$. This conclusion comes with an important caveat, however, in that other AGNs may have been present, but were heavily obscured and therefore too faint to be seen in X-rays. Absent such a population, the observational evidence for the dominant source of ionizing radiation at $z \gtrsim 6$ is beginning to favor a combination of bright galaxies at intermediate redshifts (e.g., Madau et al. 1999; Gnedin 2000; Wyithe & Loeb 2003; Meiksin 2005; Trac & Cen 2007; Faucher-Giguère et al. 2008; Gilmore et al. 2009; Vanzella et al. 2010) and dwarf galaxies ($M \lesssim 10^9\ M_\odot$) filling the distribution out to $z \gtrsim 10-12$ (e.g., Robertson & Ellis 2012; Robertson et al. 2015).

The central question then becomes whether or not the UV radiation leaking out of these galaxies is sufficient to complete the reionization process by $z \sim 6$. Direct measures of the ionizing Lyman continuum flux from galaxies at $z \gtrsim 5$ are not feasible due to the saturated hydrogen absorption by the IGM. At lower redshifts ($z \sim 3-4$), estimates are possible, but the inferred values seemingly depend on specific assumptions and mode of analysis. Nestor et al. (2011) and Mostardi et al. (2013) have concluded that the escape fraction f_{ion} may be as high as $\sim 10-15\%$, though

Vanzella et al. (2012) have questioned these numbers on the basis of significant contamination by foreground, low-redshift interlopers. An alternative approach, using spectroscopic and very deep broadband and narrowband imaging, suggests that f_{ion} may be as small as $\sim 5\%$ (Vanzella et al. 2010; Boutsia et al. 2011). The escape fraction from local galaxies may be even smaller than this, perhaps on the order of $\sim 1\%$.

However, these limits don't necessarily apply to the dwarf galaxies, which may have larger escape fractions (e.g., Fontanot et al. 2014). The dominant contributors to the cosmic reonization may therefore be these fainter galaxies extending out to $z \sim 10 - 12$ (Ferrara & Loeb 2013; Wise et al. 2014; Yue et al. 2014). The most recent work on this possibility (Robertson et al. 2015), based on the actual measured star-formation rate (SFR) history (Madau & Dickinson 2014), has concluded that an escape fraction $f_{ion} \sim 20\%$ is required in order to match the observed onset and duration of the EoR. But is such a large fraction realistic? Future work with lensing galaxy clusters to measure the Lyman continuum flux released into the IGM by gravitationally lensed, intrinsically faint galaxies may soon provide a better answer (see, e.g., Vanzella et al. 2012, Ishigaki et al. 2014).

All these uncertainties leave open the possibility that as the accuracy of the measurements improves, particularly with regard to f_{ion}, it may be difficult within the context of ΛCDM to reconcile the observed properties of the EoR with the known sources of UV ionizing radiation. Perhaps the problem is not so much the lack of adequate sources but, rather, the amount of time available within the interval $6 \lesssim z \lesssim 15$ for the reionization to have been completed. In other words, if this tension persists, it may be an indicator that the redshift-age relationship predicted by the standard model is not consistent with the properties of the EoR.

A precedent for such a proposal has already been set by the apparent early emergence of supermassive black holes at $z \gtrsim 6$ (Melia 2013a) and $\sim 10^9\ M_\odot$ galaxies at $z \sim 10 - 12$ (Melia 2014a), the very objects now thought to be responsible for the reionization. In the concordance model, the Universe was simply not old enough by $z \sim 6$ and $z \sim 12$, respectively, for such objects to have formed. One of the principal goals of this paper is therefore to examine how the requirements on f_{ion} might change when the onset and duration of the EoR are matched to the predictions of an alternative FRW cosmology known as the $R_{\rm h} = ct$ Universe (Melia 2007, 2013b, 2015b; Melia & Shevchuk 2012).

In recent years, we have carried out many comparative tests between $R_{\rm h} = ct$ and ΛCDM, showing that the data tend to favor the former with a likelihood $\sim 90\%$ versus $\sim 10\%$, according to the Akaike (AIC) and Bayesian (BIC) Information Criteria (see, e.g., Wei et al. 2013; Melia & Maier 2013; Melia 2014b, 2015a; Wei et al. 2014a, 2014b; Wei et al. 2015a, 2015b; Melia et al.

2015). Quite significantly in the context of this paper, the $R_{\rm h} = ct$ cosmology completely mitigates the tension created by the otherwise early appearance of high-redshift quasars and dwarf galaxies, because in this cosmology the EoR started at ~ 800 Myr ($z \sim 15$) and ended at $t \sim 1.89$ Gyr (i.e., $z \sim 6$), providing just the right amount of time for these structures to have grown according to standard astrophysical principles as we know them (Melia 2013a, 2014).

In this paper, we will take as our starting point the most recent constraints established for the sources of UV ionizing radiation, the measured star-formation rate as a function of redshift, and current limits on the optical depth through the IGM, and compare in detail the various contributions to the ionized filling factor in the $R_{\rm h} = ct$ and ΛCDM cosmologies. In our analysis, we include both models because significant progress has already been achieved in tracking the EoR in ΛCDM, so it should be easier to understand the differences between the two expansion scenarios. In the relevant redshift range $6 \lesssim z \lesssim 15$, these models differ not only in their predicted age-redshift relationship, but also in their comoving volumes and corresponding densities. So to fully appreciate the different outcomes, particularly with regard to the required value of f_{ion}, we will consider each effect separately, and then track the overall ionized fraction as a function of redshift. We begin with an accounting of these model differences in § 2, and provide an overview of reionization in § 3. We solve the governing equations and apply observational constraints to limit our paramter space in § 4 and § 5, and provide a discussion of our results in § 6. A summary of our conclusions is presented in § 7.

2 PRINCIPAL DIFFERENCES BETWEEN ΛCDM AND $R_{\rm H} = CT$

A proper analysis of the history of reionization in the IGM requires knowledge of both the ionization rate and recombination time as functions of t. The former is primarily dependent on the star-forming galaxy density, while the latter depends on the physical conditions in the IGM. Both of these quantities are cosmology dependent, so we begin by reviewing the relevant differences between these two models. Throughout this work, we adopt the most recent *Planck* (Ade et al. 2014) parameters for ΛCDM: $H_0 = 67.74\,{\rm km\,s^{-1}\,Mpc^{-1}}$, $\Omega_m = 0.309$, $\Omega_b h^2 = 0.02230$, $Y_p = 0.2453$, and $w_{de} = -1$, where Y_p is the Helium fraction by mass and w_{de} represents the dark-energy equation-of-state. The ratios $\Omega_m \equiv \rho_m(t_0)/\rho_c$ and $\Omega_b \equiv \rho_b(t_0)/\rho_c$ are defined in terms of today's (luminous plus dark) matter and baryon densities, respectively, and the critical density

$$\rho_c \equiv \frac{3H_0^2}{8\pi G} = 1.8785 \times 10^{-29}\, h^2\ {\rm g\,cm^{-3}}\,. \tag{1}$$

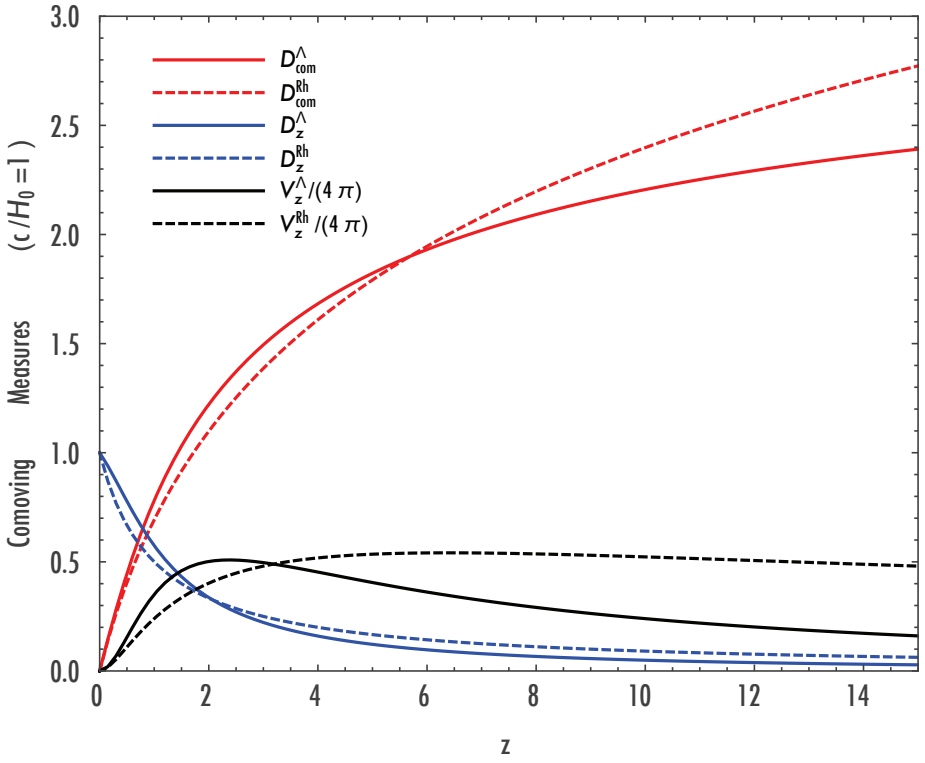

Figure 1. A comparison of various distance measures as functions of z in ΛCDM and the $R_h = ct$ Universe.

The CMB fluctuations have not yet been fully analyzed in the context of $R_h = ct$ (but see Melia 2014b, 2015), so the parameters in this model have not yet been optimized in this fashion. To keep the comparison as simple as possible, however, we will assume the same values for H_0 and Y_p, since these have been established observationally using several means. We will discuss how the other parameters differ below.

2.1 Comoving Distance and Volume

The comoving distances in ΛCDM and $R_h = ct$ are given, respectively, by the expressions

$$D_{\rm com}^{\Lambda} = \frac{c}{H_0}\int_0^z \frac{du}{\sqrt{\Omega_m(1+u)^3 + \Omega_r(1+u)^4 + \Omega_\Lambda(1+u)^{3+3w_{de}}}}\ , \tag{2}$$

and

$$D_{\rm com}^{R_h} = \frac{c}{H_0}\ln(1+z)\ . \tag{3}$$

From these, it is straightforward to calculate $D_z \equiv dD_{\rm com}/dz$ and the comoving differential volume $V_z \equiv dV_{\rm com}/dz = 4\pi D_{\rm com}^2\, dD_{\rm com}/dz$, all of which are shown as functions of redshift in figure 1.

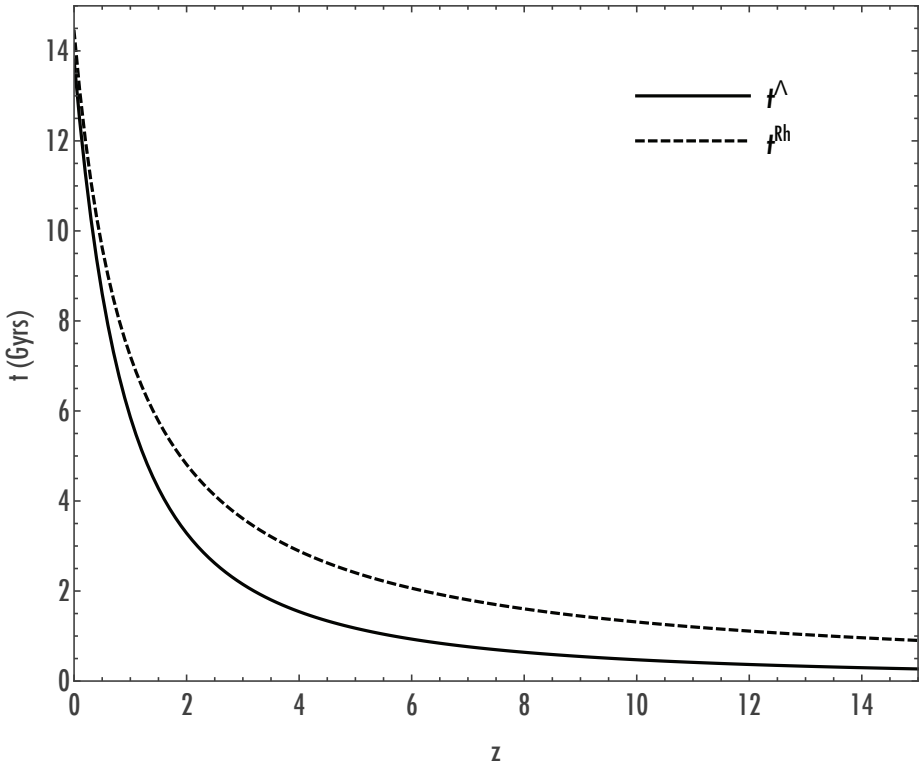

Figure 2. The age-redshift relationship for ΛCDM and the $R_\mathrm{h} = ct$ Universe.

2.2 The Age-Redshift Relationship

The age of the Universe at redshift z in ΛCDM is

$$t^{\Lambda}(z) = \frac{1}{H_0}\int_z^{\infty} \frac{du}{\sqrt{\Omega_m(1+u)^5 + \Omega_r(1+u)^6 + \Omega_\Lambda(1+u)^{5+3w_{de}}}}\ . \tag{4}$$

The corresponding expression in $R_\mathrm{h} = ct$ is

$$t^{R_\mathrm{h}}(z) = \frac{1}{H(z)}\ , \tag{5}$$

where $H(z) = H_0(1+z)$. The quantities t^{Λ} and t^{R_h} are plotted in figure 2. In addition, we show in figure 3 the ratios $R_t(z) \equiv t^{R_\mathrm{h}}/t^{\Lambda}$ and $R_V(z) \equiv V_z^{R_\mathrm{h}}/V_z^{\Lambda}$ as functions of z. These are among the most important influences affecting the ionization rate and recombination time in these two cosmologies, which we will describe in greater detail shortly.

2.3 Baryon density

Certainly up to redshift $z \sim 15$, it is safe to assume in ΛCDM that matter evolves independently of the other components in the cosmic fluid, specifically radiation and dark energy, though some questions have been raised concerning the possible instability, or creation, of dark matter. One typically takes the simplest approach in this regard, to ignore such effects, and assume that both

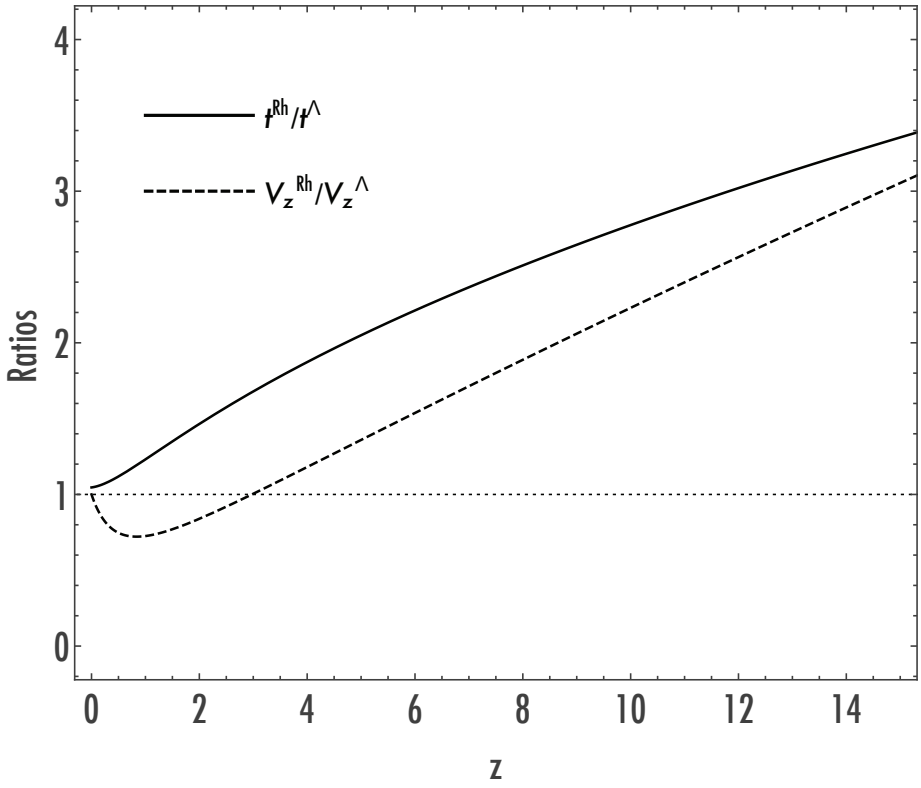

Figure 3. Ratio of differential volumes R_V and ratio of ages R_t as functions of z in ΛCDM and $R_h = ct$.

ρ_m and ρ_b scale inversely with proper volume in this model, meaning that

$$\begin{aligned} \rho_m^{\Lambda} &= \Omega_m \rho_c (1+z)^3 \,, \\ \rho_b^{\Lambda} &= \Omega_b \rho_c (1+z)^3 \,. \end{aligned} \tag{6}$$

The corresponding comoving densities $\overline{\rho}_m^{\Lambda} \equiv \Omega_m \rho_c$ and $\overline{\rho}_b^{\Lambda} = \Omega_b \rho_c$ are constant in z. The comoving Hydrogen number density is therefore given by the expression

$$\overline{n}_H^{\Lambda} = \frac{(1-Y_p)\Omega_b \rho_c}{m_H} = 1.89 \times 10^{-7}\,\mathrm{cm}^{-3} \,. \tag{7}$$

The comoving number density of electrons $\overline{n}_e^{\Lambda} = f_e Q \overline{n}_H^{\Lambda}$ depends on the ionization state of the medium, where Q is the ionization fraction of Hydrogen, and f_e is a correction factor that accounts for the ionization of Helium. For simplicity, we assume that Helium is either singly ionized or doubly ionized, so that

$$f_e = 1 + \xi \frac{Y_p}{4(1-Y_p)} \,, \tag{8}$$

where we take $\xi = 1$ for $z > 4$ and $\xi = 2$ for $z \leqslant 4$ (Kuhlen & Faucher-Ginguére 2012).

The situation is a little different in the $R_h = ct$ Universe. The overall dynamics in this cosmology has been tested with a wide range of observations, from cosmic chronometers (Melia & Maier 2013) and Type Ia SNe (Wei et al. 2015a) in the local Universe, to young quasars (Melia

2013a) and the CMB (Melia 2014b, 2015a) at high redshifts, but the detailed behavior of individual components in the cosmic fluid is only now beginning to be studied, using the kind of approach discussed in this paper. The reason for this dichotomy is that, unlike ΛCDM in which the expansion dynamics can be surmised only from the properties of the individual constituents, the principal constraint in $R_{\rm h} = ct$ is the zero active mass condition, $\rho + 3p = 0$, where ρ and p are, respectively, the total energy density and pressure in the cosmic fluid (Melia 2007, 2015b; Melia & Shevchuk 2012). For many applications, particularly when it comes to calculating the expansion rate and other observable quantities, such as the luminosity distance and the redshift dependent Hubble constant $H(z)$, one does not need to know the detailed makeup of this fluid, since all of its components must together always produce a total equation-of-state $p = -\rho/3$, for which

$$\rho^{R_{\rm h}} = \rho_c(1+z)^2 \ . \tag{9}$$

When the evolution of individual components is needed (as is the case here), several conservation laws and reasonable assumptions delimit their behavior. At least in the local Universe and within the EoR, it is reasonable to assume (1) that the radiation evolves independently of matter and dark energy; (2) that (baryonic plus dark) matter exerts an insignificant pressure compared to radiation and dark energy; and (3) that the equation-of-state parameter $w_{\rm de} \equiv p_{\rm de}/\rho_{\rm de}$ for dark energy is constant. (This is not a requirement, but appears to be the simplest assumption one can make.)

For the baryon number, however, the situation is less clear. Certainly, baryon number appears to be conserved in most interactions of the standard model, but there are important exceptions, such as the chiral anomaly (e.g., White 2004). Examples of this include sphaleron solutions to the electroweak field equations (e.g., Arnold & McLerran 1987), involved in processes that violate baryon (and lepton) number conservation. But these are thought to be rare in the local Universe; they might have been much more common in the more extreme physical conditions prevalent in the early Universe, where sphalerons would have converted baryons to antileptons and antibaryons to leptons. Baryon number conservation might also have been violated in grand unified theories, which could lead, e.g., to proton decay.

Insofar as the EoR is concerned, we will assume that this period in the evolution of the Universe was sufficiently far removed from the conditions in which baryon number conservation would have been violated, so that the baryon density remained constant in the comoving frame. (This also assumes that baryons have no additional interactions during the EoR with, e.g., the dark-energy field, when the standard model of particle physics is extended. Otherwise, these calculations will

almost certainly have to be redone.) Therefore, the expression for $\overline{n}_H^{R_h=ct}$ is identical to that for $\overline{n}_H^{\Lambda}$ in Equation (7) (though the fitted values for, e.g., Ω_b could be different). For the other quantities, we work with the following simultaneous equations describing the pertinent physics at redshifts $z \lesssim 15$:

$$\rho_{\rm de} + \rho_{\rm b} + \rho_{\rm d} + \rho_{\rm r} = \rho_{\rm c}(1+z)^2 \,, \tag{10}$$

$$w_{\rm de}\rho_{\rm de} + \frac{1}{3}\rho_{\rm r} = -\frac{1}{3}\rho_{\rm c}(1+z)^2 \,, \tag{11}$$

$$\rho_{\rm b} = \Omega_{\rm b}\rho_{\rm c}(1+z)^3 \,, \tag{12}$$

and

$$\rho_{\rm r} = \Omega_{\rm r}\rho_{\rm c}(1+z)^4 \,. \tag{13}$$

In these expressions, $\rho_{\rm d}$ is the energy density of dark matter, defined by the equation

$$\rho_{\rm m} = \rho_{\rm b} + \rho_{\rm d} \,, \tag{14}$$

and ρ_{de} and ρ_r are, respectively, the dark energy and radiation energy densities, which are scaled analogously to Ω_m and Ω_b to produce the quantities Ω_{de} and Ω_r appearing below. These equations are easily solved to produce the evolution in $\rho_{\rm de}$ and $\rho_{\rm d}$ with redshift, complementing Equations (12) and (13) for the other densities:

$$\rho_{\rm de} \approx -\frac{1}{3w_{\rm de}}\rho_{\rm c}(1+z)^2\left[1+\Omega_{\rm r}(1+z)^2\right] \,, \tag{15}$$

and

$$\rho_{\rm d} \approx \rho_{\rm c}(1+z)^2\left[2-\Omega_{\rm b}(1+z) - \frac{3w_{\rm de}-1}{3w_{\rm de}} - \frac{3w_{\rm de}-1}{3w_{\rm de}}\Omega_{\rm r}(1+z)^2\right] \,. \tag{16}$$

Today's CMB temperature ($T_0 \approx 2.72$ K) translates into a normalized radiation energy density $\Omega_{\rm r} \approx 5\times10^{-5}$. Therefore, $w_{\rm de}$ must be $\sim -1/2$ in order to produce a partitioning of the constituents in line with what we see in the local Universe. With this value,

$$\Omega_{\rm de} \approx -\frac{1}{3w_{\rm de}} \approx \frac{2}{3} \,, \tag{17}$$

while

$$\Omega_{\rm m} \approx \frac{1+3w_{\rm de}}{3w_{\rm de}} \approx \frac{1}{3} \tag{18}$$

where, of course, $\Omega_{\rm m} = \Omega_{\rm b} + \Omega_{\rm d}$. Therefore, according to Equation (16), $\rho_{\rm d}(z) \to 0$ at $(1+z) \approx 15.6$. At this redshift, which we will call z_*, a dark-energy equation of state parameter $w_{\rm de} = -1/2$ would yield $\rho_{\rm de} \sim 0.68\,\rho(z_*)$, $\rho_{\rm m} = \rho_{\rm b} \sim 0.31\,\rho(z_*)$, and $\rho_{\rm r} \sim 0.01\,\rho(z_*)$. The overlap of z_* with the redshift at which the EoR is thought to have started may simply be coincidental; it's not at all obvious why these two should be linked. On the other hand, it might be interesting to speculate on possible

physical reasons (beyond the standard model) for such a correlation, though this kind of probe lies beyond the scope of the present paper.

The data we are considering in this paper do not tell us much about what is happening beyond z_*, so long as the medium at these high redshifts is neutral (up to recombination). However, we point out for future reference that, in $R_{\rm h} = ct$, a redshift $(1+z_*) = 15.6$ corresponds to a cosmic age $t_* \equiv 1/H_0(1+z_*) \approx 950$ Myr, assuming a Hubble constant $H_0 = 67.74$ km s^{-1} Mpc^{-1}. Several of the above expressions and assumptions may not be valid at times earlier than this. We do know that baryon number cannot be conserved during this epoch, because otherwise $\rho_{\rm b}/\rho \to 1$ well short of the big bang (from Equations 9 and 12). It is likely that at these early times the Universe may have been dominated by radiation and dark energy. In that case, one would have

$$\rho_{\rm de} \approx \frac{2}{1-3w_{\rm de}}\rho_{\rm c}(1+z)^2 \quad (z \gg z_*)\,, \tag{19}$$

and

$$\rho_{\rm r} \approx \frac{3w_{\rm de}+1}{3w_{\rm de}-1}\rho_{\rm c}(1+z)^2 \quad (z \gg z_*)\,, \tag{20}$$

implying a relative partitioning of $\rho_{\rm de} \approx 0.8\rho$ and $\rho_{\rm r} \approx 0.2\rho$ (if $w_{\rm de}$ continues to be constant at $-1/2$ towards higher redshifts). But as we say, this discussion is merely speculation, and has no bearing on the work reported here.

3 REIONIZATION

We consider reionization from Lyman continuum photons produced in early star-forming galaxies (SFG), but note that AGNs may provide part (i.e ~ 10 %) of the reionization (Haardt & Salvaterra 2015). The time-dependent cosmic ionization rate in the comoving frame due to star forming galaxies is given by

$$\dot{\bar{n}} = f_{ion}\,(\eta\,\xi_{ion})\,\rho_{SFR}\,, \tag{21}$$

where f_{ion} is the fraction of stellar Lyman continuum photons that escape the galaxy and reionize the IGM, ρ_{SFR} is the star-formation rate (SFR) density, and $\eta\,\xi_{ion}$ is the number of Lyman continuum photons produced per second per unit SFR scaled to the fiducial value

$$\xi_{ion} = 1.38 \times 10^{53}\,{\rm ph\,s^{-1}}\,M_\odot^{-1}\,{\rm yr}\,, \tag{22}$$

through the model parameter η that takes into account the uncertainty in the photon production efficiency (Topping & Schull 2015). This expression for $\dot{\bar{n}}$ assumes that all the Lyman continuum photons escaping into the IGM end up contributing to the reionization.

We use the empirically derived expression of Robertson et al. (2015) for the star formation rate

density

$$\rho_{SFR} = a_p \frac{(1+z)^{b_p}}{1+[(1+z)/c_p]^{d_p}} \ , \tag{23}$$

and adopt their best-fit values $a_p = 0.01376\ M_\odot\ \mathrm{yr}^{-1}\ \mathrm{Mpc}^{-3}$, $b_p = 3.26$, $c_p = 2.59$ and $d_p = 5.68$. It is appropriate for us to do this because, even though the fitting parameters were obtained by folding in the optical depth determined with Planck, the fitting values change by less than 1% without the Thomson optical depth constraint. Nonetheless, it is important to note that the template given in Equation (23) was optimized for a ΛCDM-based analysis, and therefore needs to be rescaled for the $R_h = ct$ cosmology by the ratio of comoving differential volumes $(1/R_V)$ in these two models.

The determination of ρ_{SFR} also relies on a measurement of several luminosity functions used to estimate the star-formation rate itself. This means that the data used to optimize the empirical fit for ρ_{SFR} should be recalibrated for each individual cosmology. For the specific comparison between $R_\mathrm{h} = ct$ and the concordance model, however, the difference in the luminosity distances d_L between these two cosmologies is less than 20% (and typically less than 10%) over the entire range of relevant redshifts, extending well past $z = 10$. In fact, the two luminosity distances are equal at $z \sim 8$, as one can see in Fig. 3 of Melia (2015c). Whereas the angular-diameter and comoving distances, and the time histories, differ considerably between these two models, the luminosity distances themselves do not. This $\sim 10-20\%$ difference in d_L is well within the uncertainties associated with ρ_{SFR}, so we will defer the recalibration of the SFR data to future work. But we do include the much more important differences that arise between these two models through the redshift dependence of their comoving volumes, as discussed above. The original expression from Robertson et al. (2015) (solid curve), and the rescaled one for $R_\mathrm{h} = ct$ (dashed curve), are plotted in figure 4. As expected, the larger differential volume in the $R_h = ct$ universe at higher redshifts leads to a smaller density of ionizing Lyman continuum photons, which in turn acts to increase the time required to reionize the IGM. As we shall see below, however, this effect is largely offset by the age differences between the ΛCDM and $R_h = ct$ cosmologies.

An additional caveat with the use of Equation (23) from Robertson et al. (2015) is that the star-formation rate is still poorly known at very high redshifts. This expression is an empirical fit to integrated measurements based on several implicit assumptions concerning high-redshift galaxies. It presumes that the minimum galaxy luminosity is guessed correctly, and that the stellar populations are constant. It also adopts a double power-law ansatz for the history. Substantially different histories at high redshifts result from the use of similar, though distinct, techniques (see, e.g., Bouwens et al. 2015; Visbal et al. 2015; Mashian et al. 2015). Such differences suggest that

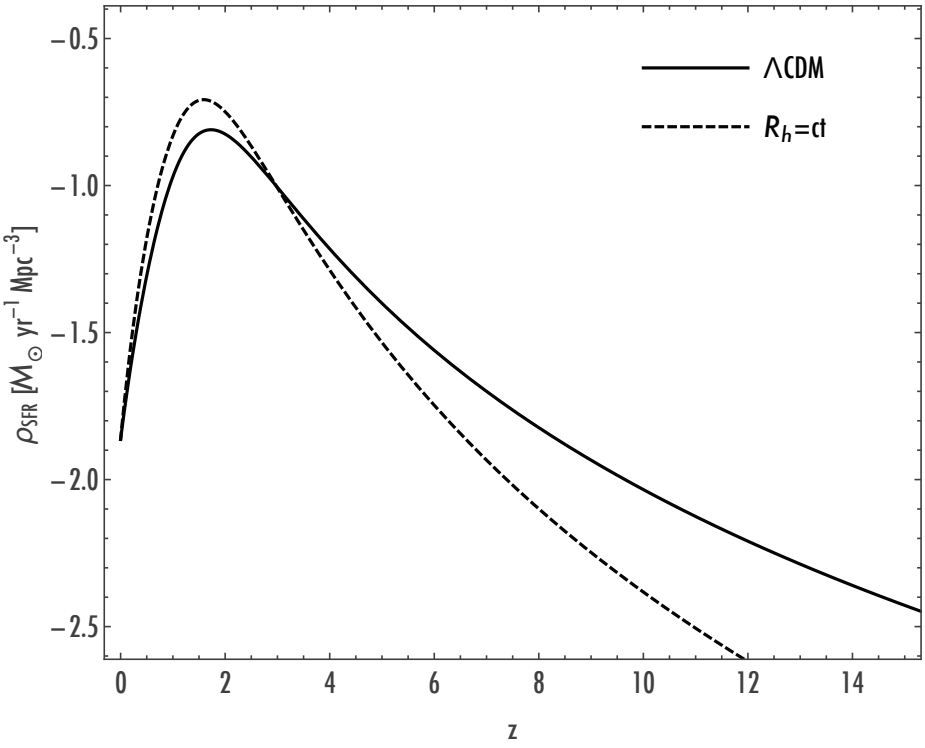

Figure 4. The star-formation rate density ρ_{SFR} versus z for ΛCDM (solid curve) and $R_h = ct$ (dashed curve), based on the empirical fit originally published by Robertson et al. (2015).

the resulting uncertainty in the reionization history is at least a factor of two, which can also affect the inferred escape fraction to a similar degree.

There are two timescales of importance in the reionization process: the characteristic ionization time $t_{ion} \equiv \bar{n}_H/\dot{\bar{n}}$, and the recombination time $t_{rec} = [C_H(z)\,\alpha_B(T)\,n_e(z)]^{-1}$, written in terms of the clumping factor C_H and recombination coefficient α_B. Note that the comoving hydrogen number density $\bar{n}_H$ has the same functional form, given in Equation (7), for both ΛCDM and $R_{\rm h} = ct$. The corresponding proper electron number density (valid for $z < z_*$, where we assume baryon conservation for both ΛCDM and $R_{\rm h} = ct$) is

$$n_e(z) = f_e\,Q\,\frac{(1-Y_p)\Omega_b\rho_c}{m_H}\,(1+z)^3\,. \tag{24}$$

We emphasize again that the numerical value given in Equation (7) assumes the fiducial ΛCDM constraint $\Omega_b h^2 = 0.02230$ for the scaled baryon density, while Ω_b is a free parameter in $R_h = ct$.

Both timescales are fairly well constrained, either through observations or on theoretical grounds, though each is subject to some uncertainty. In the case of the ionization time, the production rate of ionizing photons depends on metallicity, stellar rotation, and the initial mass function (IMF)—each of which have some variability. Various models, based on reasonable assumptions about these characteristics, produce a Lyman continuum photon production efficiency ranging between 3.22×10^{60} and 9.40×10^{60} photons per $M_\odot$ of star formation (Topping & Shull 2015), corre-

sponding to $0.74 \leqslant \eta \leqslant 2.2$. As noted in the introduction, the escape fraction of these photons has been estimated to be as small as 5% and as high as 10 - 15%; values as high as 20% appear to be necessary for ΛCDM in re-ionization studies based on the known population of dwarf galaxies at high redshifts (see, e.g., Robertson et al. 2015). Based on current understanding, we therefore explore possible outcomes within the range $0.05 \leqslant f_{ion} \leqslant 0.2$. Finally, parameters such as Ω_b have not yet been optimized in the $R_h = ct$ cosmology, though it would be reasonable to expect a value ($\lesssim 0.04$) similar to that in the standard model. For this study, we therefore adopt the range $0.01 \leqslant \Omega_b \leqslant 0.04$. As we shall see, all of these uncertainties may be incorporated into a single quantity

$$\mathcal{A} \equiv \frac{1}{\eta}\left(\frac{0.1}{f_{ion}}\right)\left(\frac{\Omega_b}{0.02}\right), \tag{25}$$

whose expected range is therefore $0.1 \leqslant \mathcal{A} \leqslant 8.2$. For example, the ionization time in the $R_h = ct$ cosmology may then be written

$$t_{ion}^{R_h=ct} = 0.38\ \mathcal{A}\, R_V(z)\left(\frac{1+[(1+z)/c_p]^{d_p}}{(1+z)^{b_p}}\right)\ \mathrm{Gyr}\ . \tag{26}$$

The corresponding expression, t_{ion}^{Λ}, for ΛCDM is identical to this, except for the omission of the R_V term: $t_{ion}^{\Lambda} = t_{ion}^{R_h=ct}/R_V(z)$.

In addition to the uncertainty in Ω_b (which appears in the expressions for $\bar{n}_H$ and n_e), the uncertainties in the recombination time arise from imprecise knowledge concerning the clumpting factor C_H, and the IGM temperature T in the recombination coefficient

$$\alpha_B = 2.59\times10^{-13}\,\mathrm{cm^3\,s^{-1}}\left(\frac{T}{10^4\,\mathrm{K}}\right)^{-0.845}\ . \tag{27}$$

For this study, we adopt the expression from Shull et al. (2012)

$$C_H(z) = C_0\left[\frac{(1+z)}{6}\right]^{-1.1} \tag{28}$$

where, following these authors, we take $C_0 = 2.9$ as a fiducial value, but also consider the range $2 \leqslant C_0 \leqslant 10$. Various applications in the literature have considered IGM temperatures between 5,000 K and 20,000 K (see, e.g., Davé et al. 2001; Smith et al. 2011), for which $0.56 \leqslant (T/10,000\ \mathrm{K})^{0.845} \leqslant 1.8$, and we will also consider this range of values here. These additional uncertainties may be combined into a second quantity

$$\mathcal{B} \equiv \left(\frac{2.9}{C_0}\right)\left(\frac{T}{10,000\,\mathrm{K}}\right)^{0.845}\left(\frac{0.02}{\Omega_b}\right), \tag{29}$$

which is expected to vary over the range $0.06 \leqslant \mathcal{B} \leqslant 5.20$. With these definitions, the recombination time in both ΛCDM and $R_h = ct$ may be written

$$t_{rec} = 70\ \frac{\mathcal{B}}{(1+z)^{1.9}}\ \mathrm{Gyr}\ , \tag{30}$$

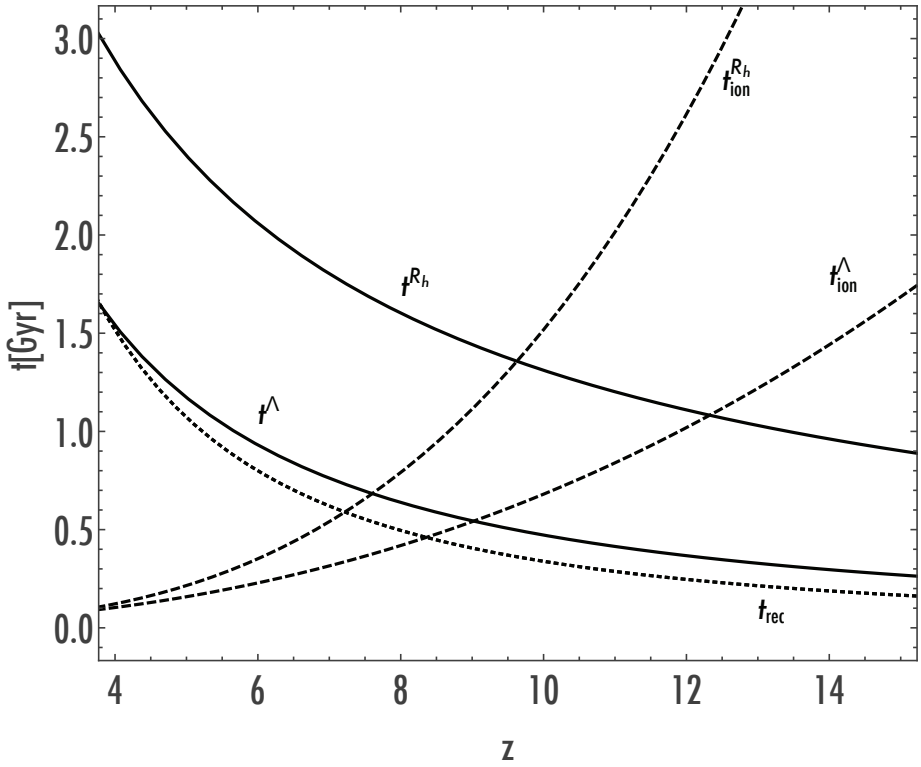

Figure 5. The age of the Universe (solid), reionization timescale (dashed), and recombination timescale (dotted), as functions of z, in ΛCDM and $R_h = ct$, assuming $\eta = 1$, $f_{ion} = 0.2$, $T = 20,000$ K, $\Omega_b = 0.0486$, and $C_0 = 4.7$. The recombination timescales are identical in these two cosmologies, so their curves overlap.

assuming $f_e = 1.081$ (for $z > 4$, where most of the reionization is thought to have occurred).

For illustration, we plot in figure 5 the ionization and recombination times in both $R_h = ct$ and ΛCDM, using parameters similar to those in Robertson et al. (2015), i.e., $\eta = 1$, $f_{ion} = 0.2$, $T = 20,000$ K and $\Omega_b = 0.02230/h^2 = 0.0486$. We mimic the constant clumping factor $C_H = 3$ used by these authors by setting $C_0 = 4.7$, which then leads to a clumping factor $C_H = 3$ at $z = 8$.[1] This choice of parameters corresponds to $\mathcal{A} = 1.2$ and $\mathcal{B} = 0.46$.

Clearly, for full reionization to occur, the Universe must be older than the reionization time ($t > t_{ion}$) which, in turn, must be shorter than the recombination time ($t_{ion} < t_{rec}$). In both cosmologies, the latter constraint is realized after the former. For these illustrative parameter values, the characteristic reionization time therefore corresponds to $z \approx 8.5$ in ΛCDM and $z \approx 7.5$ in $R_h = ct$. In the next section, we will discuss the detailed solution to the evolution equation for Q, and compare the results in these two cosmologies.

[1] Note that the expression for t_{rec} used by Robertson et al. (2015) appears to assume a fully ionized medium at all redshifts, which enhances the effect of recombination, and therefore leads to a slightly later time (i.e., a lower redshift) for reionization to be completed using our formalism.

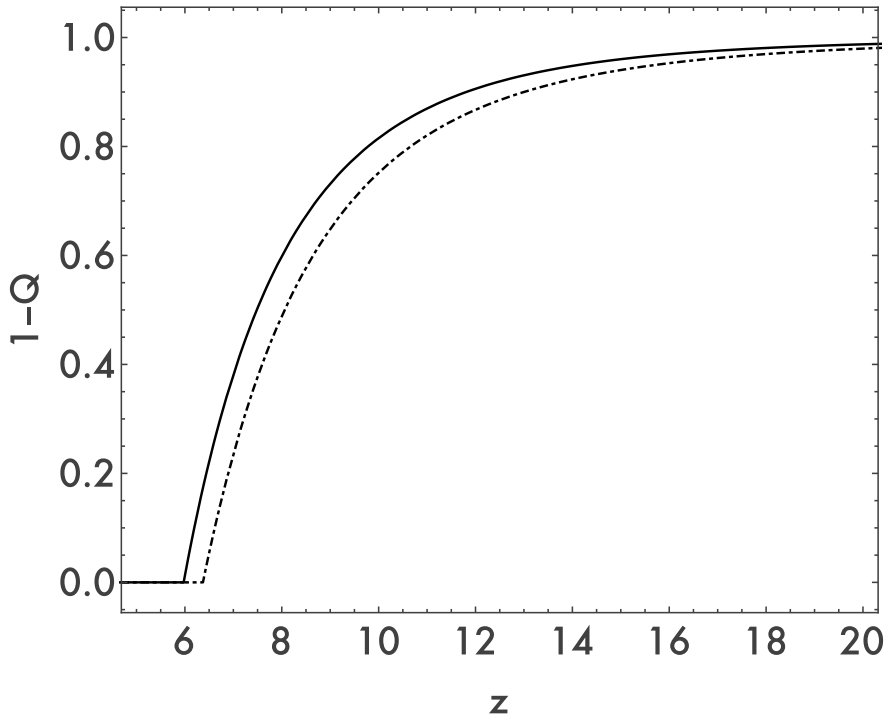

Figure 6. Reionization history for $\mathcal{A} = 1.2$ and $\mathcal{B} = 0.46$ (see figure 5): (dashed-dotted) ΛCDM; (solid) the $R_h = ct$ Universe.

4 ANALYSIS

The evolution of the IGM ionization fraction $Q(z)$ is computed by solving the differential equation

$$\frac{dQ}{dt} = \frac{\dot{\bar{n}}}{\bar{n}_H} - \frac{Q}{t_{rec}}\,, \tag{31}$$

assuming specific initial conditions, which include the value $Q = 0$ at $z = 50$ (though we note that the results are not sensitive to the initial redshift, as long as it is > 15). To understand how the differences between ΛCDM and $R_h = ct$ affect the reionization history of the Universe, we plot in figure 6 the quantity $1 - Q(z)$ versus redshift for ΛCDM (dot-dashed) and $R_\mathrm{h} = ct$ (solid), for the same values $\mathcal{A} = 1.2$ and $\mathcal{B} = 0.46$ used to generate figure 5. As expected from our discussion in §3, the reionization rate in ΛCDM steepens at $z \sim 8.5$. For $R_\mathrm{h} = ct$, the larger differential volume results in a lower star-formation rate density, and hence a longer reionization time. This effect delays reionization to lower redshifts. However, since the $R_\mathrm{h} = ct$ Universe evolves longer between $z \sim 15$ and 6 than does the standard model (i.e., 1.16 Gyrs versus 0.66 Gyrs), the volume effect is largely offset by the extra time. The net result (for this choice of $\mathcal{A}$ and $\mathcal{B}$) is that reionization in $R_\mathrm{h} = ct$ steepens at $z \sim 7.5$ and the IGM becomes fully ionized at a slightly lower redshift than in ΛCDM.

Guided by observations that indicate complete reionization occurs at $z \approx 6$, we next optimize the values of $\mathcal{A}$ and $\mathcal{B}$ for $R_\mathrm{h} = ct$ that permit reionization to end by this redshift. The results of

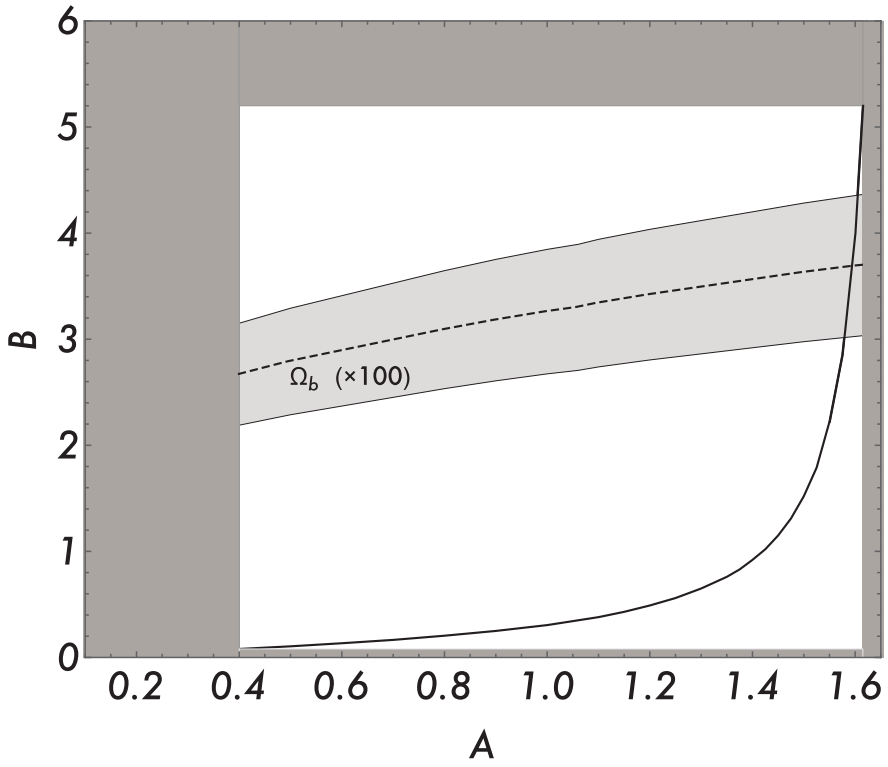

Figure 7. (Solid) The value of $\mathcal{B}$ for a given $\mathcal{A}$ that allows reionization to end by $z = 6$ in the $R_h = ct$ Universe. The horizontal dark shaded regions correspond to values of $\mathcal{B}$ outside the range $(0.06, 5.20)$, while the vertical shaded regions exclude values of $\mathcal{A}$ that similarly require a $\mathcal{B}$ outside of this range (see text). (Dashed) The corresponding value of Ω_b (as a function of $\mathcal{A}$) that yields an optical depth $\tau = 0.066$ to the scattering surface where the CMB was produced (see §5). The (light shaded) swath surrounding the dashed curve shows the uncertainty in Ω_b corresponding to the possible range in τ, i.e., $0.054 \lesssim \tau \lesssim 0.078$.

this "fitting" are presented in figure 7, where the horizontal dark gray shaded areas represent the portion of parameter space outside the range $0.06 \leqslant \mathcal{B} \leqslant 5.2$ discussed in §3. (The vertical dark gray shaded areas exclude values of $\mathcal{A}$ that would similarly correspond to $\mathcal{B}$ outside of this range.) And to bracket the possible reionization scenarios in $R_h = ct$ for all the cases under consideration, we show in figure 8 the reionization histories for the extreme values $(\mathcal{A}, \mathcal{B}) = (0.29, 0.06)$ and $(1.6, 5.2)$. Note that a longer recombination time (i.e., a larger value of $\mathcal{B}$) is offset by a longer ionization time (i.e., a larger value of $\mathcal{A}$), and longer timescales delay the onset of reionization. In other words, the solid curve in this figure demonstrates that most of the reionization for the larger values of $\mathcal{A}$ and $\mathcal{B}$ occurs at lower redshifts.

5 OPTICAL DEPTH CONSTRAINTS

In the context of ΛCDM, the integrated optical depth for Thomson scattering of the CMB provides an important constraint on the baryon density and the reionization history. The latest results published by the Planck Collaboration (2015) give a value of $\tau = 0.066 \pm 0.012$—somewhat lower than the value $\tau = 0.088 \pm 0.14$ quoted earlier by the Wilkinson Microwave Anisotropy Probe

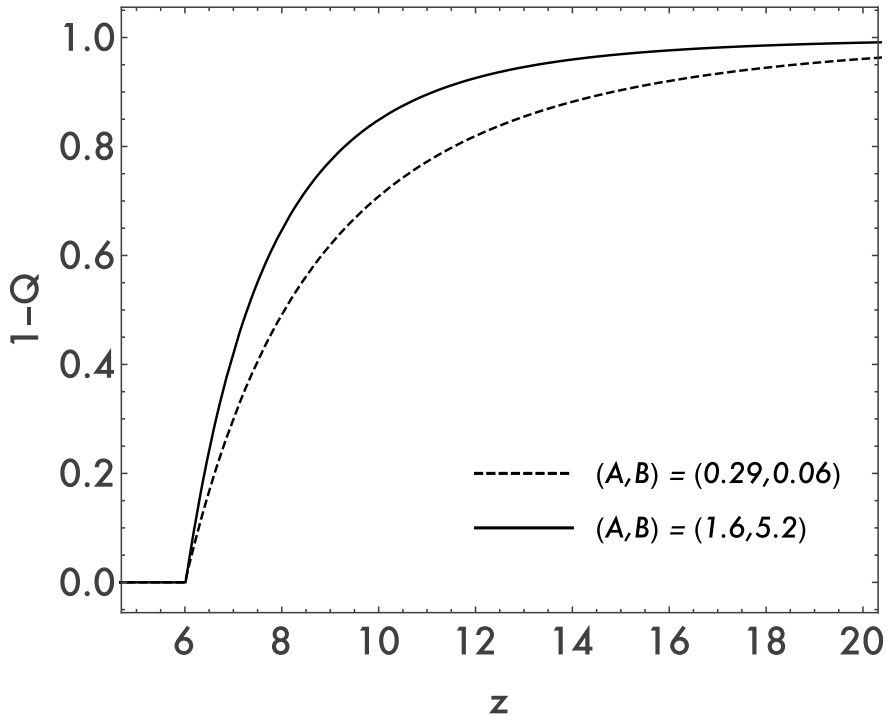

Figure 8. Reionization histories in $R_\mathrm{h} = ct$ for $(\mathcal{A}, \mathcal{B}) = (1.6, 5.2)$ (solid) and $(0.52, 0.06)$ (dashed). These bracket all the cases considered here that produce complete reionization by $z = 6$.

(Hinshaw et al. 2013). According to Robertson et al. (2015), this change in optical depth has resulted in less tension with other constraints, such as the UV escape fraction f_{ion} and the required number of galaxies at high redshift.

For the $R_\mathrm{h} = ct$ cosmology, only the "low-ell" portion of the CMB spectrum has thus far been studied in detail, principally because these moments—corresponding to angles $> 5^\circ - 10^\circ$—are influenced most directly by the expansion dynamics through the Sachs-Wolfe effect (Melia 2014b, 2015a). Conversely, the power spectrum for angles $\lesssim 1^\circ$ is generated primarily by local physics, such as the propagation of acoustic waves, and is insensitive to the background cosmology (see, e.g., Scott et al. 1995). The measurement of the scattering optical depth through the EoR is based on the interpretation of this power spectrum. Thus, because of this degeneracy in the "high-ell" spectrum among different models, and in the absence of a complete analysis for the CMB spectrum in $R_\mathrm{h} = ct$, we will for the time being simply assume that the same optical depth constraint may be applied here as in ΛCDM.

Starting with the definition $d\tau = \sigma_T\, n_e(z)\, dR$, and using the proper distance increment $dR = a\, dr = c\, dt = c\, dz(1+z)^{-1}\, H(z)^{-1}$ valid for all cosmologies, one easily obtains

$$\tau(z) = \sigma_t\, c \int_0^z \frac{n_e(z')}{H(z')(1+z')}\, dz' \,. \tag{32}$$

The correct form of $H(z)$ for each individual cosmology must then be used. In the case of $R_\mathrm{h} = ct$,

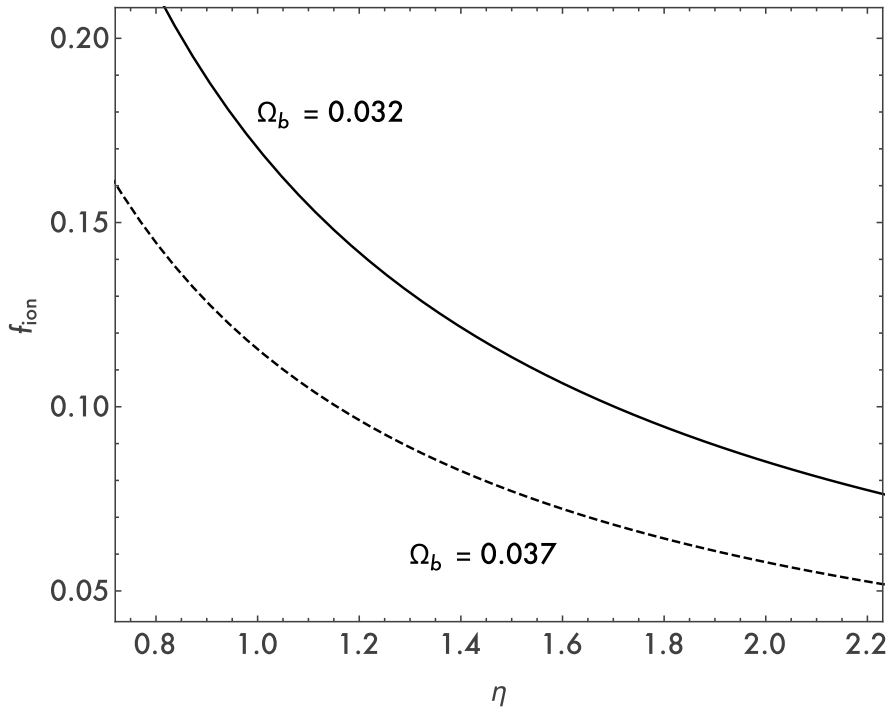

Figure 9. The escape fraction f_{ion} as a function of η, assuming a fractional baryon density $\Omega_b = 0.032$ (solid curve) and $\Omega_b = 0.037$ (dashed curve) for parameters that yield complete reionization by redshift 6, and consistent with the optical depth $\tau = 0.066$ measured by Planck.

the Hubble constant is given by the simple relation $H(z) = H_0(1 + z)$. And substituting

$$n_e(z) = f_e(z)\, Q(z)\, n_H(z) \tag{33}$$

(where here $n_H(z)$ is the proper hydrogen number density), along with

$$n_H(z) = \frac{(1 - Y_p)\Omega_b\, \rho_c}{m_H}(1 + z)^3\,, \tag{34}$$

(with $f_e = 1.081$ when $z > 4$ and 1.162 for $z \leqslant 4$), we arrive at the expression

$$\tau = 7.08 \times 10^{-4} \left(\frac{\Omega_b}{0.02}\right) \int_0^\infty f_e\, Q(z)\, (1 + z')\, dz'\,. \tag{35}$$

(Note that throughout this paper, we assume $Y_p = 0.2453$ and $h = 0.6774$.)

For a given reionization model, defined by the parameters $\mathcal{A}$ and $\mathcal{B}$, one may therefore constrain the fractional baryon density using the observationally determined optical depth. Doing this for $R_{\rm h} = ct$, using the most recent Plank measurement $\tau = 0.066$, we get the Ω_b indicated by the dashed curve in figure 7, as a function of the parameters $\mathcal{A}$ and $\mathcal{B}$ that produce complete reionization by redshift 6. The swath bracketing the dashed curve shows the possible uncertainty in Ω_b corresponding to the range in optical depth $0.054 \lesssim \tau \lesssim 0.078$. For the parameter values under consideration, we see that Ω_b in this model is restricted to the range $0.026 \lesssim \Omega_b \lesssim 0.037$. As expected from the results shown in figure 8, a higher baryon density is required to compensate for the later onset of reionization that occurs for larger values of $\mathcal{A}$ and $\mathcal{B}$.

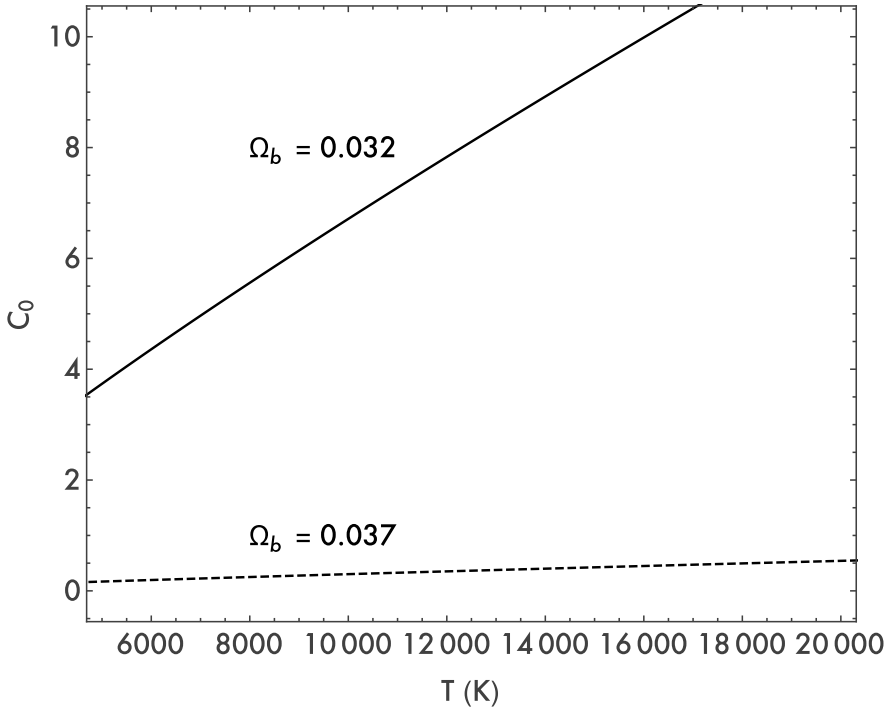

Figure 10. The clumping factor constant C_0 as a function of IGM temperature T, assuming a fractional baryon density $\Omega_b = 0.032$ (solid curve) and $\Omega_b = 0.037$ (dashed curve) for parameters that yield complete reionization by redshift 6, and consistent with the optical depth $\tau = 0.066$ measured by Planck.

6 DISCUSSION

To see how the observations of complete reionization occurring at $z = 6$ and an optical depth of $\tau = 0.066$ constrain the physical parameters under consideration, we plot in figure 9 the value of the escape fraction f_{ion} as a function of η and, in figure 10, the value of the clumping factor constant C_0 as a function of the IGM temperature T. The results are bracketed by the median value $\Omega_b = 0.032$ (solid curves: $\mathcal{A} = 0.94$ and $\mathcal{B} = 0.27$) and the highest value $\Omega_b = 0.037$ (dashed curves: $\mathcal{A} = 1.6$ and $\mathcal{B} = 5.2$) of the baryon density restricted by the range of parameters under consideration. Note that a higher baryon density, which results from higher values of $\mathcal{A}$ and $\mathcal{B}$ (see Figure 7), corresponds to the lower curves in both figures 9 and 10. The main conclusions drawn from our analysis are as follows:

1. The $R_{\rm h} = ct$ Universe predicts a different expansion rate and geometry compared to ΛCDM, but in spite of these differences, it accounts for the measured properties of the EoR quite well with physical parameter values comfortably within their expected ranges.

2. In $R_{\rm h} = ct$, the required escape fraction f_{ion} may be as high as ~ 0.2, as we find in ΛCDM, but it could also be as small as ~ 0.05. However, to achieve this lower value, one must conclude that $\Omega_b = 0.037$, $\eta = 2.2$, and that almost no clumping occurs.

3. Baryon densities lower that $\Omega_b \approx 0.03$ would seem to require large clumping factors. It is

worth noting that the $R_h = ct$ Universe is older between $z = 6 - 15$ than its ΛCDM counterpart, providing more time for clumping to occur.

7 CONCLUSION

As we have alluded to on several occasions, a principal difference between ΛCDM and $R_\mathrm{h} = ct$ is that the expansion dynamics in the former is critically dependent on the physical properties of the cosmic fluid, whereas the expansion dynamics in the latter is strictly fixed by the zero active mass condition (Melia 2015b; but see also Melia 2007 and Melia & Shevchuk 2012). Working with ΛCDM, one is therefore constrained by our imprecise knowledge concerning, e.g., the equation-of-state of dark energy. On the flip side, the relative simplicity of the observables in $R_\mathrm{h} = ct$, such as the luminosity distance and redshift dependence of the Hubble constant, has thus far made it unnecessary to study the evolution of its principal constituents. For the first time, the present paper addresses this deficiency by using measurements of the EoR to examine the evolution of the cosmic fluid in this model.

The question of how to account for the measured properties of the EoR has been subject to considerable uncertainty, first due to the unknown sources that actually contribute to the ionizing flux, but more recently due to imprecise knowledge concerning how much of this UV radiation finds its way into the IGM. The latest study by Robertson et al. (2015) suggests that the known galaxy population out to $z \sim 12$ is sufficient to complete the reionization process by redshift 6, but only if the UV escape fraction from the higher redshift dwarf galaxies is ~ 0.2, which may be somewhat larger than current estimates allow.

In this paper, the properties of the EoR have been used to probe the evolution of matter, radiation, and dark energy in $R_\mathrm{h} = ct$—not just its predicted expansion dynamics. We have argued that, at least out to a redshift ~ 15, baryons are probably conserved in the comoving frame. And with this assumption, we have shown that, consistent with the completion of reionization by redshift 6 and a scattering optical depth $\tau \sim 0.066$ measured by Planck, the required fractional baryon density falls within the "reasonable" range $0.026 \lesssim \Omega_b \lesssim 0.037$.

We have found that, in this model, an escape fraction as low as ~ 0.05 may be consistent with the measured properties of the EoR, but only if the Lyman continuum photon production is highly efficient ($\eta = 2.2$) and the baryon density is at the upper end of its expected range (i.e., $\Omega_b \sim 0.037$). This additional flexibility compared to ΛCDM is due to the different geometries

in these two models (reflected in the differential comoving volume), and different time histories (manifested through the $t(z)$ versus z relation).

This interesting result notwithstanding, we should keep in mind the important caveat that measurements of $f_{\rm ion}$ and the high-redshift star-formation rate density are still imprecise. As we have seen, both of these can significantly affect the reionization history. In galaxies where $f_{\rm ion}$ can be measured, one reliably finds only upper limits (at the level of $\sim 5-10\%$). Local galaxies may have even lower escape fractions than this. It now looks like quasars and AGNs can provide at most only $\sim 10-20\%$ of the required ionizing photons over the history of the EoR. The best candidate sources are therefore galaxies (particularly dwarf galaxies) at high redshift. Unfortunately, estimating their luminosity function is challenging since it relies heavily on the assumed minimum luminosity and their evolution with redshift, among other things. So the analysis presented in this paper should be viewed as a start of the discussion concerning the EoR in the $R_{\rm h} = ct$ Universe, but much work remains to be done, both observationally and theoretically. In particular, we point out that the properties of the EoR presented here are based primarily on the empirically determined star-formation rate and galaxy formation and evolution. Large-scale structure simulations within the $R_{\rm h} = ct$ cosmology have yet to be completed, so there is no direct evidence that this expansion scenario can create a population of galaxies consistent with the observations. The results of this extended investigation are forthcoming and will be reported elsewhere.

As of today, the $R_{\rm h} = ct$ cosmology has passed many observational tests, but almost always based on its global predictions, independent of its physical constituents. The fact that this model can also account for the EoR is an important start to the process of understanding whether or not $R_{\rm h} = ct$ is truly a viable representation of cosmic evolution. Future work should include an assessment of the fact that baryon conservation is almost certainly violated at redshifts $z > 15$, and the influence of dark energy does not disappear towards $t = 0$, as it does in the standard model. Baryon number is not conserved in ΛCDM either, but in this case, the violation is required only in the first few minutes following the big bang. In $R_{\rm h} = ct$, on the other hand, the baryon number in the comoving frame probably changes for a much longer period. In addition, dark energy cannot be a cosmological constant; it is dynamic, suggesting particle physics beyond the standard model. These two features are probably not independent of each other, but it is still too early for us to know.

ACKNOWLEDGMENTS

We are very grateful for the thoughtful and helpful comments provided by the anonymous referee. F.M. is grateful to Amherst College for its support through a John Woodruff Simpson Lectureship, and to Purple Mountain Observatory in Nanjing, China, for its hospitality while part of this work was being carried out. This work was partially supported by grant 2012T1J0011 from The Chinese Academy of Sciences Visiting Professorships for Senior International Scientists, and grant GDJ20120491013 from the Chinese State Administration of Foreign Experts Affairs. M.F. is supported at Xavier University through the Hauck Foundation.

REFERENCES

Ade, P. A. R. et al. 2014, A&A, 571, article id A23

Arnold, P. & McLerran, L., 1987, PRD, 36, 581

Barkana, R. & Loeb, A. 2001, Phys. Rep., 349, 125

Boutsia, K., Grazian, A., Giallongo, E. et al., 2011, ApJ, 736, 41

Bouwens, R. J., Illingworth, G. D., Oesch, P. A., Caruana, J., Holwerda, B., Smit, R., Wilkins, S., 2015, ApJ, 811, id.140

Bromm, V. & Larson, R. B. 2004, ARA&A, 42, 79

Fan, X., Carilli, C. L. & Keating, B., ARA&A, 44, 415

Faucher-Ciguère, C.-A., Lidz, A., Hernquist, L. & Zaldarriaga, M., 2008, ApJL, 682, L9

Ferrara, A. & Loeb, A., 2013, MNRAS, 431, 2826

Fontanot, F., Cristiani, S., Pfrommer, C., Cupani, G. & Vanzella, E., 2014, MNRAS, 438, 2097

Gilmore, R. C., Madau, P., Primack, J. R., Somerville, R. S. & Haardt, F., 2009, MNRAS, 399, 1694

Gnedin, N. Y., 2000, ApJ, 535, 530

Haardt, F. & Madau, P., 1996, ApJ, 461, 20

Hinshaw, G., Larson, D., Komatsu, E. et al., 2013, ApJS, 208, 19

Ishigaki, M., Kawamata, R., Ouchi, M., Oguri, M., Kazuhiro, S. & Ono, Y., 2014, ApJ, submitted (arXiv:1408.6903)

Jarosik, N., Bennett, C. L., Dunkley, J. et al., 2011, ApJS, 192, 14

Kuhlen, M. & Faucher-Giguére, C. -A. 2012, MNRAS, 423, 862

Madau, P. & Dickinson, M., 2014, ARA&A, 52, 415

Madau, P., Haardt, F., & Rees, M. J. 1999, ApJ, 514, 648

Madau, F. & Salvaterra, R., 2015, A&A Letters, submitted (arXiv:1502.03089)

Mashian, N., Sturm, E., Sternberg, A., Janssen, A., Hailey-Dunsheath, S., Fischer, J., Contursi, A., González-Alfonso, E., Graciá-Carpio, J., Poglitsch, A., Veilleux, S., Davies, R., Genzel, R., Lutz, D., Tacconi, L., Verma, A.; Weiss, A., Polisensky, E. and Nikola, T., 2015, ApJ, 802, id.81

Meiksin, A., 2005, MNRAS, 356, 596

Melia, F., 2007, MNRAS, 382, 1917

Melia, F., 2013a, ApJ, 764, 72

Melia, F., 2013b, A&A, 553, id A76

Melia, F., 2014a, AJ, 147, 120

Melia, F., 2014b, A&A, 561, id. A80

Melia, F., 2015a, AJ, 149, 6

Melia, F., 2015b, CQG, submitted

Melia, F., 2015c, Astrop. & Sp. Sci., 356, 393

Melia, F. & López Corredoira, M. 2015, ApJ, submitted (arXiv:1503.05052)

Melia, F. & Maier, R. S., 2013, MNRAS, 432, 2669

Melia, F. & Shevchuk, A.S.H., 2012, MNRAS, 419, 2579

Melia, F., Wei, J.-J. & Wu, X.-F., 2015, AJ, 149, 2

Miralda-Escude, J. & Ostriker, J. P., 1990, ApJ, 350, 1

Mostardi, R. E., Shapley, A. E., Nestor, D. B., Steidel, C. C., Reddy, N. A. & Trainor, R. F., 2013, ApJ, 779, 65

Nestor, D. B., Shapley, A. E., Steidel, C. C. & Siana, B., 2011, ApJ, 736, 18

Planck Collaboration, 2015, arXiv:1502.01589

Robertson, B. E. & Ellis, R. S., 2012, ApJ, 744, 95

Robertson, B. E., Ellis, R. S., Furlanetto, S. R. & Dunlop, J. S., 2015, ApJL, 802, L19

Scott, D., Silk, J. and White, M., 1995, Science, 268, 829

Songaila, A., AJ, 127, 2598

Topping, M. W. & Shull, M. J., 2015, ApJ, 800, 97

Trac, H. & Cen, R., 2007, ApJ, 671, 1

Vanzella, E., Siana, B., Cristiani, S. & Nonino, M., 2010, MNRAS, 404, 1672

Vanzella, E., Guo, Y., Giavalisco, M. et al., 2012, ApJ, 751, 70

Visbal, E., Haiman, Z. and Bryan, G. L., 2015, MNRAS, 453, 4456

Wei, J.-J., Wu, X.-F. & Melia, F., 2013, ApJ, 772, id. 43

Wei, J.-J., Wu, X.-F. & Melia, F., 2014a, ApJ, 788, id. 190

Wei, J.-J., Wu, X.-F., Melia, F., Wei, D.-M. & Feng, L.-L., 2014b, MNRAS, 439, 3329

Wei, J.-J., Wu, X.-F., Melia, F. & Maier, R. S., 2015a, AJ, 149, 102

Wei, J.-J., Wu, X.-F. & Melia, F., 2015b, MNRAS, 447, 479

White, A. R., 2004, PRD, 69, 096002

Wise, J. H., Demchenko, V. G., Halicek, M. T., Norman, M. L., Turk, M. J., Abel, T. & Smith, B. D., 2014, MNRAS, 442, 2560

Wyithe, J.S.B. & Loeb, A., 2003, ApJ, 586, 693

Yue, B., Ferrara, A., Vanzella, E. & Salvaterra, R., 2014, MNRAS, 443, L20